Fabrication and Characterization of In$_{0.9}$Ga$_{0.1}$O EGFET pH Sensors

Chia-Hsun Chen [1,*], **Shu-Bai Liu** [2,3] **and Sheng-Po Chang** [2,3,*]

1   Department of Optometry, Chung Hwa University of Medical Technology, Tainan 71703, Taiwan
2   Institute of Microelectronics, Department of Electrical Engineering, National Cheng Kung University, Tainan 70101, Taiwan; shu.bai.liu@gmail.com
3   Advanced Optoelectronic Technology Center, National Cheng Kung University, Tainan 70101, Taiwan
*   Correspondence: chen1985ch@mail.hwai.edu.tw (C.-H.C.); changsp@mail.ncku.edu.tw (S.-P.C.); Tel.: +886-6-3367163 (C.-H.C.)

Abstract: In this study, the In$_{0.9}$Ga$_{0.1}$O sensing membrane were deposited by using the RF magnetron sputtering at room temperature and combined with commercial MOSFETs as the extended gate field effect transistor (EGFET) pH sensors. The sensing performance of the In$_{0.9}$Ga$_{0.1}$O EGFET pH sensors were measured and analyzed in the pH value of range between 2 to 12. In the saturation region, the pH current sensitivity calculated from the linear relationship between the I_{DS} and pH value was approximately 56.64 μA/pH corresponding to the linearity of 97.8%. In the linear region, the pH voltage sensitivity exhibited high sensitivity and linearity of 43.7 mV/pH and 96.3%, respectively. The In$_{0.9}$Ga$_{0.1}$O EGFET pH sensors were successfully fabricated and exhibited great linearity. The analyzed results indicated that the In$_{0.9}$Ga$_{0.1}$O was a robust material as a promising sensing membrane and effectively used for pH sensing detection application.

Keywords: extended gate field effect transistor; In$_{0.9}$Ga$_{0.1}$O sensing membrane

1. Introduction

The pH sensors have widely attracted attention and been used for biological and chemical applications, such as biosensors [1–3], the medical community [4–6], and clinical measurements [7]. Since the first ion-sensitive field-effect transistor (ISFET) was fabricated by Bergveld in 1970 [8], several teams in the world have studied to improve the sensing performance of the ISFET [9–11]. To avoid the device contact with solution, the structure of extended gate field-effect transistor (EGFET) was invented by J. Van Der Spiegel et al. in 1983 [12,13]. This structure was developed for the disadvantages of ISFET. Instead of the sensing region separated from the FET and connected through a wire, the EGFET has the following advantages over ISFET, such as the transistor could be reused, the extended gate contact to the sensing membrane through the wire could reduce the risk of ESD damaging the transistor, and the light-induced damage of the devices can also be reduced [14]. The distinction between ISFET and EGFET is that the metal gate of MOSFET is replaced by a high resistivity sensing membrane. Compared with the ISFET, the EGFET also operates through adjusting the concentration of absorbed ions residing on the surface, which caused the electrical signal variation between the sensing membrane and buffer solution. Therefore, the EGFET is a useful structure for detecting several reactions in various applications. The EGFET pH sensors have become processes compatible, convenient, and stable regard to light and outside temperature [15,16]. Recently, several materials were developed and used on the EGFET pH sensors as the sensing membranes, such as zinc oxide (ZnO) [17], titanium dioxide (TiO$_2$) [18], ruthenium oxide (RuO$_x$) [19], and vanadium oxide (V$_2$O$_5$) [20], but scientist still develop more materials for the application. More recently, indium gallium oxide (InGaO) was also found to be a robust material as a promising sensing membrane due to its inherent properties, including wide bandgap, and can be

deposited at room temperature [21,22]. Moreover, indium gallium oxide (InGaO) has been used in various applications, such as thin-film transistors (TFT) [23], electrolyte–insulator–semiconductor [24], and solar-blind photodetectors [22]. Among these device applications, the InGaO thin-film transistors were based on their high stability and field-effect mobility, and the solar-blind photodetector has the advantage of adjustable broadened detection range between 3.5 eV to 4.9 eV. According to the bandgap of 3.5 eV of In_2O_3, it can properly combine with the Ga_2O_3 with a bandgap of 4.9 eV [22,23]. However, the InGaO extended gate field-effect transistor (EGFET) has never been published in previous literature, even though InGaO is a robust material for using as a sensing membrane. In this paper, we investigated the characteristics of the material and the device application of EGFETs fabricated by the InGaO alloy deposited by radio frequency (RF) magnetron sputtering. To measure the sensing properties of the InGaO sensing membrane, we constructed EGFETs by connecting the InGaO sensing membrane to a commercial MOSFET. The commercial MOSFET CD4007UB is manufactured by Texas Instruments. The electronic characteristics were discussed in detail.

2. Materials and Methods

The schematic configuration of InGaO extended gate field-effect transistor (EGFET) is shown in Figure 1. Before deposition of the InGaO sensing membrane, the quartz substrates were prepared by the following processes. First, the quartz substrates were placed in the ultrasonic oscillator and sequentially rinsed with acetone, methanol, and DI water, respectively. Next, the substrates were then dried by N_2 gas and deposited 70 nm titanium conductive film by using E-beam evaporation to serve as a contact electrode. To assure the sensing membrane quality and prevent the influence by other impurities, the chamber was necessarily evacuated to a background pressure of 10^{-6} torr by a high vacuum pump before processing. The 300 nm InGaO sensing membrane were deposited on the Ti (70 nm)/quartz substrates by RF magnetron sputtering at room temperature, using InGaO ceramic sputtering targets (atomic ratio In:Ga = 9:1, 99.99% purity). According to the sputtering targets, the atomic ratio of indium to gallium was 9:1, the InGaO sensing membrane was represented by $In_{0.9}Ga_{0.1}O$. During $In_{0.9}Ga_{0.1}O$ deposition, the base pressure, deposited pressure, and RF sputtering power, gas flow ratios of $O_2/(O_2 + Ar)$ were kept at 3×10^{-6} Torr, 5 mTorr, 100 W, and 20%, respectively. The distance between Ti (70 nm)/quartz substrate holder and target gun was 9 cm, and the angle between the gun and the holder was 30°. The holder was rotated at a speed of 10 rotations per minute to lead the good uniformity of sensing membrane thickness distribution. The completed sensing membrane was connected to the gate of the commercial MOSFETs (CD4007UB) with wire. In order to avoid leakage current, the devices were packaged by epoxy to prevent the reaction between titanium and solution. The size of the sensing widow of 1 cm×1 cm was defined and packaged by using the epoxy resin. To measure the sensing performances of the $In_{0.9}Ga_{0.1}O$ EGFET pH sensors, the encapsulated devices and the reference electrode (Ag/AgCl) were immersed together in the electrolytic solution of the various pH values. The pH value of the electrolytic solution was varied from 2 to 12, which depended on the concentration of the H^+ ions. The measuring system constructed by Agilent 4156C semiconductor parameter analyzer was used to verify the performance of the $In_{0.9}Ga_{0.1}O$ EGFET pH sensors. The whole system was shown in Figure 2.
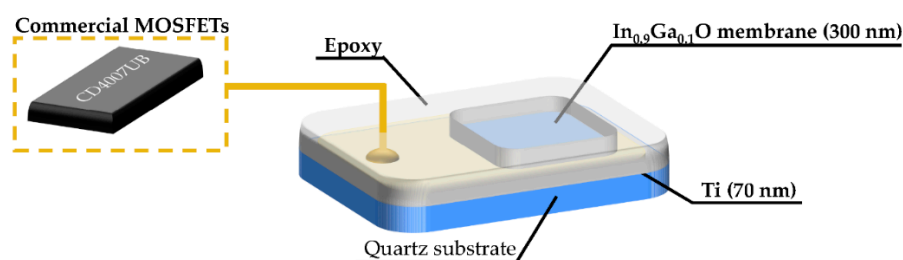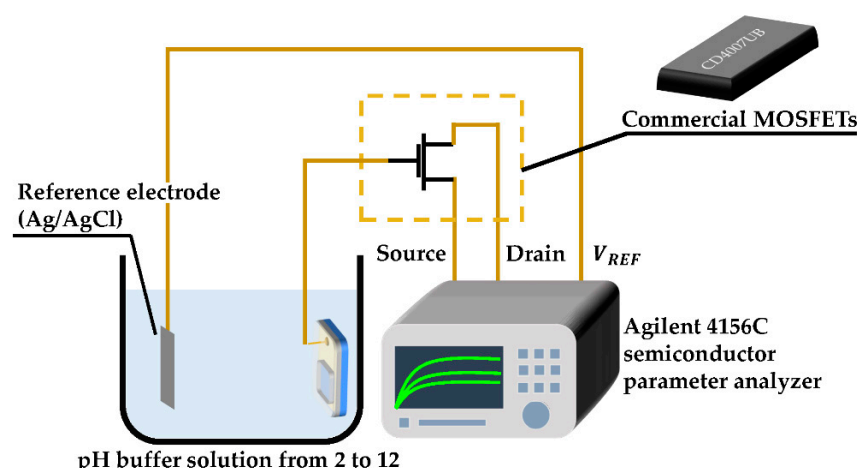

Figure 1. Schematic diagram of sensing structure.

Figure 2. Measurement system of the $In_{0.9}Ga_{0.1}O$ EGFET pH sensors.

3. Results and Discussion

To investigate the material characteristics of the $In_{0.9}Ga_{0.1}O$ sensing membrane, a thickness of 75 nm $In_{0.9}Ga_{0.1}O$ thin film was deposited on a quartz substrate to serve as the test sample. Figure 3a,b showed the surface morphologies of the $In_{0.9}Ga_{0.1}O$ sensing membrane. Figure 3a was the top-view image measured by the field emission scanning microscope (FESEM) operated at 10 keV. It was observed the $In_{0.9}Ga_{0.1}O$ sensing membrane exhibited a uniform surface, indicating that the film was deposited with good thickness uniformity by the RF-sputtering system. As shown in Figure 3b, the surface roughness was measured by AFM, with a scanning area of 5 μm × 5 μm. The root mean square surface roughness obtained was 1.088 nm. Furthermore, in the aspect of elemental analysis, secondary-ion mass spectrometry (SIMS) was used to reveal the signal intensity of all the elements, including indium (In), gallium (Ga), and oxygen (O). As shown in Figure 4, the stable intensity of In, Ga, and O along the z-direction indicated the uniform distribution of these elements in the $In_{0.9}Ga_{0.1}O$ sensing membrane.
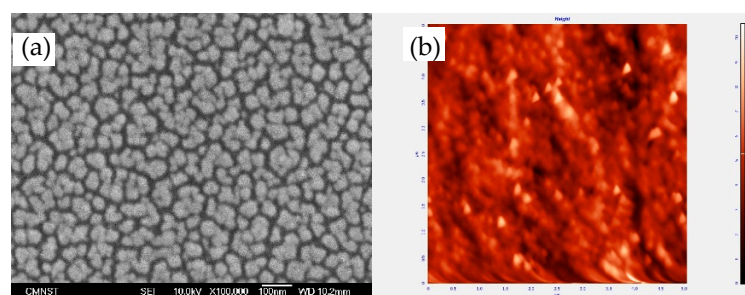

Figure 3. The top-view images of (**a**) FESEM and (**b**) AFM of the $In_{0.9}Ga_{0.1}O$ sensing membrane.

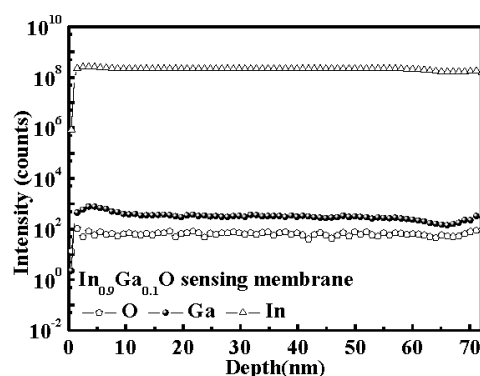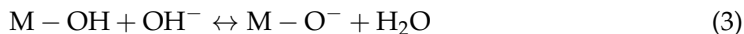**Figure 4.** The SIMS profile of the $In_{0.9}Ga_{0.1}O$ sensing membrane.

The drain current (I_{DS}) and drain–source voltage (V_{DS}) varied with the pH value, which can be obtained by the basic MOSFET expressions. Figure 5 shows the I_{DS}–V_{DS} characteristics of the $In_{0.9}Ga_{0.1}O$ EGFET pH sensors operated at a reference voltage (V_{REF}) of 3 V with the value of pH buffer solution from 2 to 12. For understanding the I_{DS}–V_{DS} characteristics of the $In_{0.9}Ga_{0.1}O$ EGFET pH sensors in the saturation region, the I_{DS}–V_{DS} curve can be expressed as the following equation [25,26]:

$$I_{DS} = \frac{\mu_n C_{ox}}{2} \times \frac{W}{L}\left[\left(V_{REF} - V_{T(EGFET)}\right)^2\right] \tag{1}$$

where μ_n is the electron mobility, C_{ox} is the gate capacitance per unit area, W/L is the channel width to length ratio, $V_{T(EGFET)}$ is the threshold voltage of the $In_{0.9}Ga_{0.1}O$ EGFET pH sensors. As shown in Figure 5, the drain current operated in the saturation region increased with decreasing value of pH buffer solution. The drain current of the $In_{0.9}Ga_{0.1}O$ EGFET pH sensors operated at a reference voltage (V_{REF}) of 3 V affected by the H^+ ions concentration. The amphoteric reaction between the $In_{0.9}Ga_{0.1}O$ membranes surface and pH buffer solutions can be realized by the site-binding model theory. The metal-OH groups were formed by the dangling bond that resided on the surface of $In_{0.9}Ga_{0.1}O$ membrane. When the $In_{0.9}Ga_{0.1}O$ membrane is immersed in the pH buffer solutions, the metal-OH groups can accept or donate a proton led the surface charge accreted. In the low pH value, it denotes the high accretion of H^+ ions on the sensing membrane in acidic solution and provided positive charge (OH_2^+). Conversely, the high pH value denotes the high accretion of OH^- ions on the sensing membrane in alkali solution and provided negative charge (O^-). The protonation and deprotonation mechanism can be expressed as following equation [27–29]:

$$M - OH + H^+ \leftrightarrow M - OH_2^+ \tag{2}$$

$$M - OH + OH^- \leftrightarrow M - O^- + H_2O \tag{3}$$

The surface potential voltage (φ) of the $In_{0.9}Ga_{0.1}O$ EGFET pH sensors between $In_{0.9}Ga_{0.1}O$ membrane and pH buffer solutions can be expressed as the following equation by the site-binding model and double layer theory [24,30]:

$$\varphi = 2.303\frac{KT}{q}\frac{\beta}{\beta + 1}\left(pH_{pzc} - pH\right) \tag{4}$$

where pH_{pzc} is the pH value at the point of zero charge, K is Boltzmann's constant, T is the absolute temperature, q is the elementary charge, and β is the sensitivity parameter. The sensitivity parameter dependent on the various factors, including the H^+ ions concentration and the surface sites of the $In_{0.9}Ga_{0.1}O$ membrane, it could be expressed as following equation [24,31]:

$$\beta = \frac{2q^2 N_s (K_a K_b)^{1/2}}{kT C_{DL}} \tag{5}$$

where N_s is the total number of sensing sites per area, K_a and K_b are the acid and base equilibrium constants and C_{DL} is the capacitance of the electric double layer at the $In_{0.9}Ga_{0.1}O$ membrane/pH buffer solutions interface. The sensing mechanism of the $In_{0.9}Ga_{0.1}O$ membrane surface/pH buffer solutions interface could be described by using the Gouy–Chapman–Stern mode [32]. When the $In_{0.9}Ga_{0.1}O$ EGFET pH sensors were immersed in the pH buffer solutions interface, the cations and anions were distributed between the reference electrode (Ag/AgCl) and $In_{0.9}Ga_{0.1}O$ membrane. The electric double layer was formed on the interface and composed of space charge from the electrolyte. The capacitance (C_{DL}) value dependent on the reaction of ions absorption and desorption from the electric double layer. In general, the pH sensing properties of EGFET pH sensors affected by the surface potential voltage (φ). According to the reason mentioned above, the drain current (I_{DS}) in saturation region (V_{DS} = 3 V) shift downward with increasing pH value was obtained and shown in Figure 6. To find the properties of the $In_{0.9}Ga_{0.1}O$ EGFET pH sensors, the

pH current sensitivity could be derived from the linear relation between the drain-source current and the pH value. As shown in the Figure 6, the derived pH current sensitivity of the optimized and reproduction device was approximately 56.64 µA/pH and 53.30 µA/pH, corresponding to the linearity of 97.8% and 99.8%, respectively.
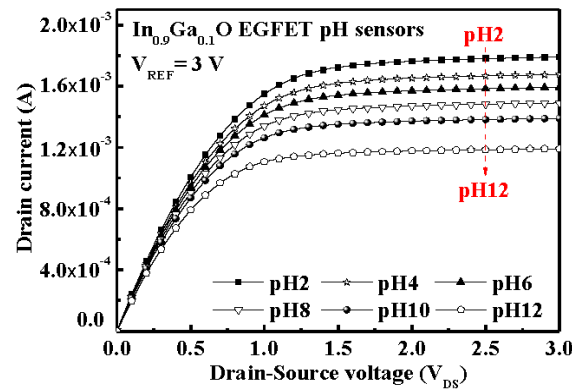

Figure 5. The drain current (I_{DS}) and drain–source voltage (V_{DS}) of the In$_{0.9}$Ga$_{0.1}$O EGFET pH sensors.
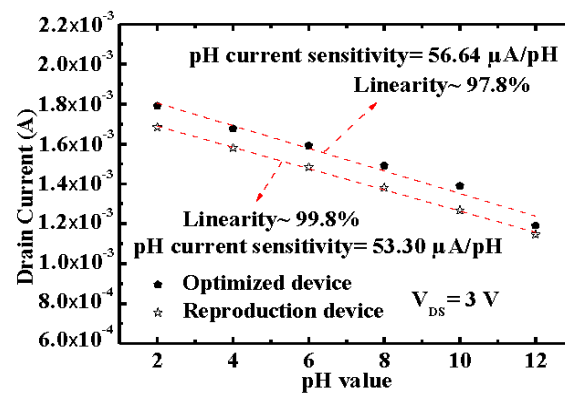

Figure 6. The drain current (I_{DS}) as a function of pH value.

Figure 7 reveals the transfer characteristic curves ($I_{DS}-V_{REF}$) characteristics of the In$_{0.9}$Ga$_{0.1}$O EGFET pH sensors with the pH value from 2 to 12 at a fixed drain–source voltage of 0.3 V. The $I_{DS}-V_{REF}$ characteristics of the In$_{0.9}$Ga$_{0.1}$O EGFET pH sensors in the linear region can be expressed as following equation [26]:

$$I_{DS} = \frac{\mu_n C_{ox}}{2} \times \frac{W}{L} \left[2 \left(V_{REF} - V_{T(EGFET)} \right) V_{DS} - V_{DS}^2 \right] \tag{6}$$

where V_{DS} is the drain to source voltage, $V_{T(EGFET)}$ is the threshold voltage and it can be expressed in the following equation [26]:

$$V_{T(EGFET)} = V_{T(MOSFET)} - \frac{\varphi_M}{q} + E_{REF} + \chi^{Sol} - \varphi \tag{7}$$

where $V_{T(MOSFET)}$ is the threshold voltage of the commercial MOSFET, φ_M is the work function of the metal gate relative to the vacuum level, E_{REF} is the potential of the reference electrode, χ^{Sol} is the surface dipole potential of the solvent, and φ is the surface potential voltage at In$_{0.9}$Ga$_{0.1}$O membrane/pH buffer solutions interface. As shown in Figure 7, the threshold voltage ($V_{T(EGFET)}$) shifted to a higher voltage (V_{REF}) as the pH value increased, which was consistent with the site-binding model. According to the site-binding model, the H$^+$ and metal-OH groups of the In$_{0.9}$Ga$_{0.1}$O membrane surface attracted with each other by the hydroxyl bond to protonated, leading to the surface potential increased with increasing H$^+$ ions in acid. Therefore, the threshold voltage ($V_{T(EGFET)}$) decreased with

increasing surface potential. Contrarily, deprotonated reaction happened while the pH value of buffer solution increased, where the increased OH^- will combine with metal-OH. The deprotonation led to the threshold voltage ($V_{T(EGFET)}$) shift toward the higher bias with increasing the pH value. To find the properties of the $In_{0.9}Ga_{0.1}O$ EGFET pH sensors, the pH voltage sensitivity can be extracted from the transfer characteristic curves ($I_{DS}-V_{REF}$) characteristics and expressed as the following equation [18]:

$$\text{pH voltage sensitivity} = \frac{\Delta V_{T(EGFET)}}{\Delta\text{pH}} \qquad (8)$$

Figure 8 reveals the characteristics of V_{REF} versus pH value derived in the linear region of the $I_{DS}-V_{REF}$ curve at a fixed V_{DS} of 0.3 V and I_{DS} of 200 μA. The values of V_{REF} were 1.65 V, 1.75 V, 1.80 V, 1.88 V, 1.96 V, and 2.12 V for various pH values range from 2 to 12, respectively. As shown in Figure 8, the pH voltage sensitivity of the $In_{0.9}Ga_{0.1}O$ EGFET pH sensors was estimated to be 43.7 mV/pH and the corresponding linearity was revealed about 96.3%. It was observed the positive correlation between V_{REF} and pH value and exhibited great linearity.
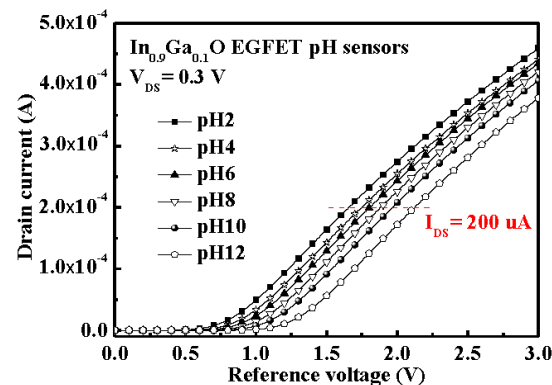

Figure 7. The transfer characteristic curves ($I_{DS}-V_{REF}$) characteristics of the $In_{0.9}Ga_{0.1}O$ EGFET pH sensors.
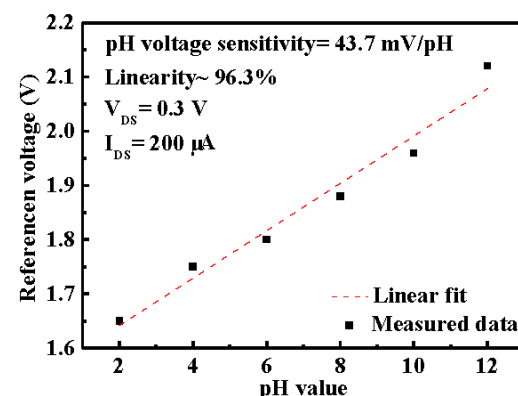

Figure 8. Reference voltage (V_{REF}) as a function of pH value.

In general, the pH voltage sensitivity depend on the surface potential is limited to the value of 59 mV/pH at room temperature, which was based on the Nernst response [33]. Here, we summarized the EGFET pH sensor performance of the $In_{0.9}Ga_{0.1}O$ and other sensing membranes in previous study in Table 1. As shown in Table 1, P. D Batista et al. used the zinc oxide (ZnO) film as the sensing layer and the sensitivity was 38 mV/pH [17]. The sensitivity of CuS thin films reported by F. A. Sabah et al. and showed improved sensitivity of 37 mV/pH by using the structure of the CuS/ITO membrane [34,35]. E. M. Guerra et al. investigated the sensing performance of vanadium oxide/hexadecylamine

(V$_2$O$_5$/HDA) membrane and presented a voltage sensitivity of 38.1 mV/pH [20]. Compared to the previous device fabricated by using various materials as the sensing membrane, the In$_{0.9}$Ga$_{0.1}$O membrane used in this work and revealed good properties was one of the potential materials as the sensing membrane of EGFET pH sensors. To realize In$_{0.9}$Ga$_{0.1}$O membrane properties for pH sensing application, the stability of the In$_2$O$_3$ based and InGaO based sensing membrane was published in the previous study [24,36]. The In$_2$O$_3$ based pH-EGFET was reported by B. R. Huang et al., it confirms the immediate response of the pH was changed from 2 to 12 in steps of 2 pH units [36]. The stability of InGaO based electrolyte-insulator-semiconductor (EIS) was reported by C. H. Kao et al. [24], it was evaluated with pH sequence of 7, 4, 7, 10, and 7. As the previous results, it indicated that the compound fabricated by the material of the indium oxide and gallium oxide were promising materials for the pH value detection for various type device applications.

Table 1. Comparison of the sensitivity of the EGFET pH sensors based on various structures and sensing membranes.

Sample	pH Current Sensitivity	Linearity	pH Voltage Sensitivity	Linearity	pH Range	Ref.
ZnO	NA	NA	38 mV/pH	NA	2 to 12	[33]
CuS	25 μA/pH	96.9%	23 mV/pH	96.5%	2 to 12	[34]
CuS/ITO	37 μA/pH	99.3%	37 mV/pH	98.5%	2 to 12	[35]
V$_2$O$_5$/HDA	NA	NA	38.1 mV/pH	NA	2 to 12	[19]
In$_{0.9}$Ga$_{0.1}$O	56.64 μA/pH	97.8%	43.7 mV/pH	96.3%	2 to 12	This work

4. Conclusions

In this study, we deposited the In$_{0.9}$Ga$_{0.1}$O membrane with RF magnetron sputtering at room temperature and successfully applied it to be the sensing film in the structure of the extended gate field-effect transistor (EGFET). To demonstrate the properties of the In$_{0.9}$Ga$_{0.1}$O EGFET pH sensors, the devices were immersed in the pH buffer solution and measured the variation of current and voltage to calculate device sensitivity. In the saturation region, the pH current sensitivity calculated from the linear relationship between the I$_D$ and pH value was approximately 56.64 μA/pH, corresponding to the linearity of 97.8%. In the linear region, the pH voltage sensitivity exhibited higher sensitivity and linearity of 43.7 mV/pH and 96.3%, respectively. These results reveal that the In$_{0.9}$Ga$_{0.1}$O EGFET pH sensors could accurately respond to the protonation and deprotonation by the metal-OH groups resided on the In$_{0.9}$Ga$_{0.1}$O sensing membrane in the different pH values.

References

1. Koike, K.; Sasaki, T.; Hiraki, K.; Ike, K.; Hirofuji, Y.; Yano, M. Characteristics of an extended gate field-effect transistor for glucose sensing using an enzyme-containing silk fibroin membrane as the bio-chemical component. *Biosensors* **2020**, *10*, 1–13. [CrossRef] [PubMed]

2. Kwon, J.; Lee, B.H.; Kim, S.Y.; Park, J.Y.; Bae, H.; Choi, Y.K.; Ahn, J.H. Nanoscale FET-based transduction toward sensitive extended-gate biosensors. *ACS Sens.* **2019**, *4*, 1724–1729. [CrossRef]

3. Danielson, E.; Sontakke, V.A.; Porkovich, A.J.; Wang, Z.; Kumar, P.; Ziadi, Z.; Yokobayashi, Y.; Sowwan, M. Graphene based field-effect transistor biosensors functionalized using gas-phase synthesized gold nanoparticles. *IEEE Sens. J.* **2016**, *16*, 6496–6514.

4. Kang, B.S.; Wang, H.T.; Ren, F.; Pearton, S.J.; Morey, T.E.; Dennis, D.M.; Johnson, J.W.; Rajagopal, P.; Roberts, J.C.; Piner, E.L.; et al. Enzymatic glucose detection using ZnO nanorods on the gate region of AlGaN/GaN high electron mobility transistors. *Appl. Phys. Lett.* **2007**, *91*, 252103. [CrossRef]

5. Chen, C.P.; Ganguly, A.; Lu, C.Y.; Chen, T.Y.; Kuo, C.C.; Chen, R.S.; Tu, W.H.; Fischer, W.B.; Chen, K.H.; Chen, L.C. Ultrasensitive in situ label-free DNA detection using a GaN nanowire-based extended-gate field-effect-transistor sensor. *Anal. Chem.* **2011**, *83*, 1938–1943. [CrossRef] [PubMed]

6. Campos, R.; Borme, J.M.; Guerreiro, J.R.; Machado, G., Jr.; Cerqueira, M.F.; Petrovykh, D.Y.; Alpuim, P. Attomolar label-free detection of DNA hybridization with electrolyte-gated graphene field-effect transistors. *ACS Sens.* **2019**, *4*, 286–293. [CrossRef]

7. Palit, S.; Singh, K.; Lou, B.S.; Her, J.L.; Pang, S.T.; Pan, T.M. Ultrasensitive dopamine detection of indium-zinc oxide on PET flexible based extended-gate field-effect transistor. *Sens. Actuators B* **2020**, *310*, 127850. [CrossRef]

8. Bergveld, P. Development of an ion-sensitive solid-state device for neurophysiological measurements. *IEEE. Trans. Biomed. Eng.* **1970**, *17*, 70–71. [CrossRef]

9. Keeble, L.; Moser, N.; Manzano, J.R.; Georgiou, P. ISFET-based sensing and electric field actuation of DNA for on-chip detection: A review. *IEEE Sens. J.* **2020**, *20*, 11044–11065. [CrossRef]

10. Bellando, F.; Mele, L.J.; Palestri, P.; Zhang, J.; Ionescu, A.M.; Selmi, L. Sensitivity, noise and resolution in a BEOL-modified foundry-made ISFET with miniaturized reference electrode for wearable point-of-care applications. *Sensors* **2021**, *21*, 1779. [CrossRef] [PubMed]

11. Cho, S.K.; Cho, W.J. Ultra-high sensitivity pH-sensors using silicon nanowire channel dual-gate field-effect transistors fabricated by electrospun polyvinylpyrrolidone nanofibers pattern template transfer. *Sens. Actuators B* **2021**, *326*, 128835. [CrossRef]

12. van der Spiegel, J.; Lauks, I.; Chan, P.; Babic, D. The extended gate chemically sensitive field effect transistor as multi-species microprobe. *Sens. Actuators A* **1983**, *4*, 291–298. [CrossRef]

13. Li, H.H.; Dai, W.S.; Chou, J.C.; Cheng, H.C. An extended-gate field-effect transistor with low-temperature hydrothermally synthesized SnO_2 nanorods as pH sensor. *IEEE Electron Device Lett.* **2012**, *33*, 1495–1497. [CrossRef]

14. Baldi, A.; Bratov, A.; Mas, R.; Dominguez, C. Electrostatic discharge sensitivity tests for ISFET sensors. *Sens. Actuators B* **2001**, *80*, 255–260. [CrossRef]

15. Pullano, S.A.; Critello, C.D.; Mahbub, I.; Tasneem, N.T.; Shamsir, S.; Islam, S.K.; Greco, M.; Fiorillo, A.S. EGFET-based sensors for bioanalytical Applications: A Review. *Sensors* **2018**, *18*, 4042. [CrossRef]

16. Young, S.J.; Lai, L.T.; Tang, W.L. Improving the performance of pH sensors with one-dimensional ZnO nanostructures. *IEEE Sens. J.* **2019**, *19*, 10972–10976. [CrossRef]

17. Batista, P.D.; Mulato, M. ZnO extended-gate field-effect transistors as pH sensors. *Appl. Phys. Lett.* **2005**, *87*, 143508. [CrossRef]

18. Yang, C.C.; Chen, K.Y.; Su, Y.K. TiO_2 nano flowers based EGFET sensor for pH sensing. *Coatings* **2019**, *9*, 251. [CrossRef]

19. Tanumihardja, E.; Olthuis, W.; Van den Berg, A. Ruthenium oxide nanorods as potentiometric pH sensor for organs-on-chip purposes. *Sensors* **2018**, *18*, 2901. [CrossRef]

20. Guerra, E.M.; Mulato, M. Synthesis and characterization of vanadium oxide/hexadecylamine membrane and its application as pH-EGFET sensor. *J. Sol. Gel. Sci. Technol.* **2009**, *52*, 315–320. [CrossRef]

21. Chen, K.Y.; Hsu, C.C.; Yu, H.C.; Peng, Y.M.; Yang, C.C.; Su, Y.K. The effect of oxygen vacancy concentration on indium gallium oxide solar blind photodetector. *IEEE Trans. Electron. Devices* **2018**, *65*, 1817–1822. [CrossRef]

22. Chang, T.H.; Chang, S.J.; Weng, W.Y.; Chiu, C.J.; Wei, C.Y. Amorphous indium–gallium–oxide UV photodetectors. *IEEE Photon. Technol. Lett.* **2015**, *27*, 2083–2086. [CrossRef]

23. Yang, C.P.; Chang, S.J.; Chang, T.H.; Wei, C.Y.; Juan, Y.M.; Chiu, C.J.; Weng, W.Y. Thin-film transistors with amorphous indium-gallium-oxide bilayer channel. *IEEE Electron. Device Lett.* **2017**, *38*, 572–575. [CrossRef]

24. Kao, C.H.; Liu, C.S.; Xu, C.Y.; Lin, C.F.; Chen, H. Ti-doped indium gallium oxide electrolyte–insulator–semiconductor membranes for multiple ions and solutes detectors. *J. Mater. Sci. Mater. Electron.* **2019**, *30*, 20596–20604. [CrossRef]

25. Bergveld, P. The impact of MOSFET-based sensors. *Sens. Actuators A* **1985**, *8*, 109–127. [CrossRef]

26. Das, A.; Ko, D.H.; Chen, C.H.; Chang, L.B.; Lai, C.S.; Chu, F.C.; Chow, L.; Lin, R.M. Highly sensitive palladium oxide thin film extended gate FETs as pH sensor. *Sens. Actuators B* **2014**, *205*, 199–205. [CrossRef]

27. Sharma, P.; Gupta, S.; Singh, R.; Ray, K.; Kothari, S.L.; Sinha, S.; Sharma, R.; Mukhiya, R.; Awasthi, K.; Kumar, M. Hydrogen ion sensing characteristics of Na_3BiO_4–Bi_2O_3 mixed oxide nanostructures based EGFET pH sensor. *Int. J. Hydrogen Energy* **2020**, *45*, 18743–18751. [CrossRef]

28. Yates, D.E.; Levine, S.; Healy, T.W. Site-binding model of the electrical double layer at the oxide/water interface. *J. Chem. Soc.* **1973**, 1807–1818. [CrossRef]

29. Yusof, K.A.; Rahman, R.A.; Zulkefle, M.A.; Herman, S.H.; Abdullah, W.F.H. EGFET pH sensor performance dependence on sputtered TiO_2 sensing membrane deposition temperature. *J. Sens.* **2016**, *10*, 7594531.

30. Lin, C.F.; Kao, C.H.; Lin, C.Y.; Liu, C.S.; Liu, Y.W. Comparison between performances of In_2O_3 and In_2TiO_5-based EIS biosensors using post plasma CF_4 treatment applied in glucose and urea sensing. *Sci. Rep.* **2019**, *9*, 3078. [CrossRef]

31. Pan, T.M.; Huang, M.D.; Lin, C.W.; Wu, M.H. Development of high-k $HoTiO_3$ sensing membrane for pH detection and glucose biosensing. *Sens. Actuators B* **2010**, *144*, 139–145. [CrossRef]

32. Brüesch, P.; Christen, T. The electric double layer at a metal electrode in pure water. *J. Appl. Phys.* **2004**, *95*, 2846–2856. [CrossRef]

33. Burke, L.D.; Whelan, D.P. A voltammetric investigation of the charge storage reactions of hydrous iridium oxide layers. *J. Electroanal. Chem.* **1984**, *162*, 121–141. [CrossRef]

34. Sabah, F.A.; Ahmed, N.M.; Hassan, Z.; Almessiere, M.A. Effect of light on the sensitivity of CuS thin film EGFET implemented as pH sensor. *Int. J. Electrochem. Sci.* **2016**, *11*, 4380–4388. [CrossRef]

35. Sabah, F.A.; Ahmed, N.M.; Hassan, Z.; Hardan, N.H.A. Sensitivity of CuS and CuS/ITO EGFETs implemented as pH sensors. *Appl. Phys. A* **2016**, *122*, 839-1–839-6. [CrossRef]

36. Huang, B.R.; Hung, S.C.; Lo, Y.P. Effects of In_2O_3 modification of sprayed multiwalled carbon nanotubes for pH-sensing applications. *Mater. Sci. Semicond. Process.* **2014**, *26*, 710–715. [CrossRef]